# Vortex depinning frequency in $YBa_2Cu_3O_{7-x}$ superconducting thin films: Anisotropy and temperature dependence

M. Golosovsky, M. Tsindlekht, H. Chayet, and D. Davidov
*Racah Institute of Physics, Hebrew University of Jerusalem, Israel*
(Received 4 March 1994)

We have used the parallel-plate resonator technique to study the microwave surface resistance $R_s$ and the penetration depth $\lambda$ of $YBa_2Cu_3O_{7-x}$ thin epitaxial films at 5.5 GHz in the presence of magnetic field $H \leq 0.8$ T and at 30 K $< T <$ 80 K. The magnetic-field dependence of $R_s$ and $\lambda$ allows determination of the vortex viscosity $\eta$, pinning constant $\alpha$, and depinning frequency $\omega_0$ for different field orientations. To the best of our knowledge, this is among the first measurements of the angular dependence of $\eta$, $\alpha$, and $\omega_0$. We find that the angular dependences of $\eta$, $\alpha$, and $\omega_0$ are fairly well described by the scaling model of Blatter, Geshkenbein, and Larkin. We demonstrate that (i) the temperature dependence of $\eta$ is well described by the Bardeen-Stephen model with reduced normal-state resistivity, (ii) the pinning constant is close to its upper limit at lowest temperatures and decreases exponentially with increasing temperature, and (iii) the depinning frequency is of the order of 10 GHz, almost orientation independent and weakly depends on temperature. We analyze the values of the depinning frequency for different type-II superconductors and demonstrate that it is directly related to the quasiparticle scattering rate.

## I. INTRODUCTION

When a vortex line in a type-II superconductor oscillates under the influence of an alternating current its motion is limited by frictional and pinning forces. The simplest description of the linear vortex dynamics is given by the equation of motion suggested by Gittleman and Rosenblum:[1]

$$\eta\dot{x} + \alpha x = J\Phi_0 , \tag{1}$$

where $J$ is the driving current density, $x$ is the vortex displacement, $\alpha$ is the pinning constant (Labusch parameter), $\eta$ is the viscous drag coefficient (viscosity), and $\Phi_0$ is the flux quantum. One can show that Eq. (1) leads to the vortex resistivity

$$\rho_v = \frac{\Phi_0 H}{\eta} \frac{1}{(1 + i\omega_0/\omega)} , \tag{2}$$

where

$$\omega_0 = \frac{\alpha}{\eta} . \tag{3}$$

Examination of Eq. (1) indicates that pinning forces dominate at low frequencies while frictional forces dominate at high frequencies. The depinning (crossover) frequency $\omega_0$ delineates between the low- and high-frequency regimes. At $\omega \gg \omega_0$ vortex resistivity is real, $\rho_v = H\Phi_0/\eta$, and the vortex motion is highly dissipative, while at $\omega \ll \omega_0$ vortex resistivity is imaginary, $\rho_v = i\omega H\Phi_0/\alpha$, and the vortex motion is almost nondissipative. The depinning frequency is also closely related to the attempt frequency that determines flux creep.[2,3] Hence, $\omega_0$ is a very important parameter of the vortex dynamics. The depinning frequency was found to be in the MHz range for several low-$T_c$ superconductors.[1,4] There are very few experimental studies of high-frequency vortex dynamics in oxide superconductors which indicate that for these materials $\omega_0$ is in the microwave range.[5-12]

For low-$T_c$ superconductors the depinning frequency was determined by measuring the frequency dependence of the vortex dissipation.[1] This is practically impossible for high-$T_c$ superconductors because of the major difficulty to change the frequency through several orders of magnitude in the microwave range. However, it is possible to determine $\omega_0$ using Eq. (3), e.g., through simultaneous measurement of the pinning constant $\alpha$ and the viscosity $\eta$ using the same sample and experimental setup.

Several experimental studies were dedicated to the determination of either $\alpha$ (Refs. 13-15) or $\eta$ (Refs. 5-8 and 15-17) in oxide superconductors. There are, however, only few studies[11,12] in which $\alpha$ and $\eta$ were determined simultaneously for the same sample. To the best of our knowledge, the angular dependence of $\eta$, $\alpha$, and $\omega_0$ in anisotropic superconductors was not studied yet experimentally. (However, in oxide[18] and organic[19] superconductors there were studies of the angular-dependent microwave absorption which is determined by the combination of the viscosity and pinning constant.) The general scaling arguments of Blatter, Geshkenbein, and Larkin,[20] Klemm,[21] Hao and Clem,[22] Kogan and Clem[23] suggest that in the limit of individual vortices, when $\eta$ and $\alpha$ do not depend on magnetic field, their angular dependence should be the same and the depinning frequency should be orientation independent. The experimental data concerning these issues are controversial. The anisotropy of the pinning constant in $YBa_2Cu_3O_{7-x}$ single crystals[14] is in striking contradiction to the scaling arguments,[20] while the angular dependence of the vortex viscosity in $YBa_2Cu_3O_{7-x}$ thick films[16] obeys scaling arguments. Therefore, the available experimental data suggest that the depinning frequency may have strong angular depen-

 

dence in contrast to the theoretical predictions.[20] Certainly, new investigations are needed to resolve this discrepancy.

The parallel-plate resonator (PPR) technique[24] allows estimation of depinning frequency by measuring pinning constant and viscosity simultaneously. Recently, this technique was used[11] to study viscosity and pinning in thick $YBa_2Cu_3O_{7-x}$ films at moderate fields of 0.35 T and for fixed orientation of the field $H\|c$ at several temperatures. We modified the PPR technique in order to study angular dependences and to accommodate larger fields. The purpose of this paper is the systematic study of the vortex viscosity, pinning constant, and depinning frequency in thin $YBa_2Cu_3O_{7-x}$ films as function of the field orientation and temperature.

## II. METHODOLOGY

### A. Theory of operation

The parallel-plate resonator (PPR) is a very sensitive technique to measure surface resistance and surface reactance of superconductors.[24] The resonator consists of a pair of superconducting films and a thin dielectric spacer in between. The $Q$ factor of such resonator is determined by the dissipation in the superconductor, by the losses in the dielectric spacer and by radiation losses. For a resonator with sufficiently thin spacer the dissipation in the superconductor is the main source of losses. The resonant frequency of the parallel-plate resonator is given by Ref. 24 as follows:

$$f^2=\frac{c^2}{\epsilon K}\left[\left[\frac{n}{2L}\right]^2+\left[\frac{m}{2W}\right]^2\right], \tag{4}$$

where $\epsilon$ is the dielectric constant of the spacer, $L$ and $W$ are the length and width of the films, $n$ and $m$ are the mode numbers [for the fundamental mode $(n,m)=(0,1)$ or (1,0)], and $K$ is a dimensionless complex factor that accounts for the decrease of the phase velocity due to the inductance of the superconductor and is given by

$$K=1+\left[\frac{2\lambda}{s}\right]\coth\left[\frac{d}{\lambda}\right]. \tag{5}$$

Here, $s$ is the thickness of the dielectric spacer, $d$ is the film thickness and $\lambda$ is the complex penetration depth. We define the complex frequency shift as $\delta f/f=\Delta f/f+iQ^{-1}$, where $Q^{-1}$ is the loss factor of the resonator due to the dissipation in superconductor, and $\Delta f/f$ is the resonant frequency shift. Provided $|K-1|\ll 1$, the complex frequency shift is $\delta f/f=(K-1)/2$. Then Eq. (5) yields

$$\frac{\Delta f}{f}=\mathrm{Re}\left[\frac{\lambda}{s}\coth\left[\frac{d}{\lambda}\right]\right], \tag{6a}$$

$$Q^{-1}=\mathrm{Im}\left[\frac{\lambda}{s}\coth\left[\frac{d}{\lambda}\right]\right]. \tag{6b}$$

In the thick-film limit $\lambda\ll d$, Eq. (6) reduces to $\delta f/f=\lambda/s$, while in the thin-film limit $\lambda\gg d$, it reduces to $\delta f/f=\lambda^2/sd$. Using experimentally determined parameters $\Delta f/f, Q^{-1}$, and Eq. (6), one can find the real and imaginary parts of the penetration depth and calculate the surface impedance $Z_s=R_s+iX_s=i\omega\mu_0\lambda$. We note that in the thick-film limit the surface resistance $R_s$ and reactance $X_s$ are directly related to the $Q$ factor and frequency shift $\Delta f$, respectively,

$$R_s=2\pi fsQ^{-1}, \tag{7a}$$

$$X_s=2\pi s\Delta f. \tag{7b}$$

We estimate the vortex viscosity and pinning constant from the magnetic-field dependence of the penetration depth as follows. Neglecting quasiparticle skin depth, the high-frequency penetration depth in a magnetic field and not very close to $T_c$ may be written as[25] $\lambda^2(H,T)\approx\lambda_0^2(T)+\lambda_v^2(H,T)$. Here, $\lambda_v$ is the vortex penetration length (complex) and $\lambda_0$ is the London penetration length in the absence of a magnetic field. Penetration length is directly related to the resistivity $\lambda^2=i\rho/\omega\mu_0$. From Eq. (2) we find the real and imaginary parts of $\lambda_v$:

$$\mathrm{Re}(\lambda_v^2)=\frac{\Phi_0 H}{\alpha\mu_0}\frac{1}{1+(\omega/\omega_0)^2}, \tag{8a}$$

$$\mathrm{Im}(\lambda_v^2)=\frac{\Phi_0 H}{\alpha\mu_0}\frac{\omega/\omega_0}{1+(\omega/\omega_0)^2}, \tag{8b}$$

$$\frac{\mathrm{Im}(\lambda_v^2)}{\mathrm{Re}(\lambda_v^2)}=\frac{\omega}{\omega_0}. \tag{8c}$$

In the actual experiment we measure the $Q$ factor and frequency shift $\Delta f/f$ of the resonator and calculate the complex penetration depth $\lambda$ using Eq. (6). We determine $\lambda_0$, $\lambda_v$ and then we find $\omega_0$ from Eq. (8c). Using this value of $\omega_0$ we find $\alpha$ and $\eta$ from Eqs. (8a) and (8b). Note, that we do not assume *a priori* any specific field dependence of $\omega_0$, $\alpha$, and $\eta$.

The above model presents the simplest approach to the vortex dynamics. Equations (1) and (8) operate with two independent parameters $\alpha$ and $\eta$ ($\alpha$ and $\omega_0$). For their determination it is necessary to measure two independent variables, e.g., $\mathrm{Re}(\lambda_v^2)$ and $\mathrm{Im}(\lambda_v^2)$. The more complicated Coffey-Clem model[25] accounts for the flux creep and introduces an additional parameter $U_0(T)$, namely, the height of the pinning potential. This parameter can be found from the frequency dependence of $\mathrm{Re}(\lambda_v^2)$ and $\mathrm{Im}(\lambda_v^2)$. Very recently, Revenaz *et al.*[12] measured frequency dependence of the surface impedance of $YBa_2Cu_3O_{7-x}$ striplines and analyzed their data in terms of the Coffey-Clem model. Reference 12 demonstrates that while flux-creep processes in $YBa_2Cu_3O_{7-x}$ thin films might be relevant at 1 GHz, they are not that important at higher frequencies. Therefore, we work at the frequency of 5.5 GHz and use the simplest model [Eqs. (1) and (8)] with the minimal number of fitting parameters.

### B. Experimental procedure

We used the PPR technique with the following modifications.

(a) The coupling to the parallel-plate resonator is usually performed by microstrips or gradient loops.[24] These methods have some drawbacks. In fact, coupling by microstrips is not very efficient, while for gradient loop coupling there is uncertainty in the type of excitation (for square samples the fundamental mode is degenerate). Therefore, we adopted coupling with small loops (nongradient) which we placed close to the centers of the film edges in order to excite a single fundamental mode (see Fig. 1).

(b) The PPR technique was originally developed to study samples with very low surface resistance, not higher than 1-2 mΩ. For this purpose a very thin teflon spacer ($\epsilon=2$, $s=12.5$ $\mu$km) was used. This configuration is not very suitable for measurements in magnetic field because the surface resistance increases with the field and the signal disappears. Therefore, we used MgO or sapphire spacers with a higher dielectric constant $\epsilon=9.5$ and with a greater thickness $s=350$ $\mu$km, in order to accommodate larger surface resistances. The resonance frequency of such resonator with $1\times1$ cm$^2$ films is $f\approx5.5$ GHz.

A major difficulty in the PPR measurements is to recognize the proper signal. Besides the parallel-plate mode there are usually strong "stripline" modes. In such a mode the superconducting plate forms the central conductor of the stripline while the sample chamber forms a ground plane. The resonant frequency of the stripline mode is rather close to that of the parallel-plate mode and is doubly degenerate (because there are two superconducting plates). The $Q$ factor of the stripline mode is determined by the losses in the superconducting plate and in the sample chamber. Actually, this mode may be used to estimate the surface resistance of the samples close to $T_c$ when the PPR signal is very small. We distinguish between the stripline modes and PPR mode by taking out the dielectric spacer. In such a way the PPR mode disappears, while the stripline modes do not. When one of the superconducting plates is taken out, the PPR mode and one of the stripline modes disappear, while the second stripline mode does not.

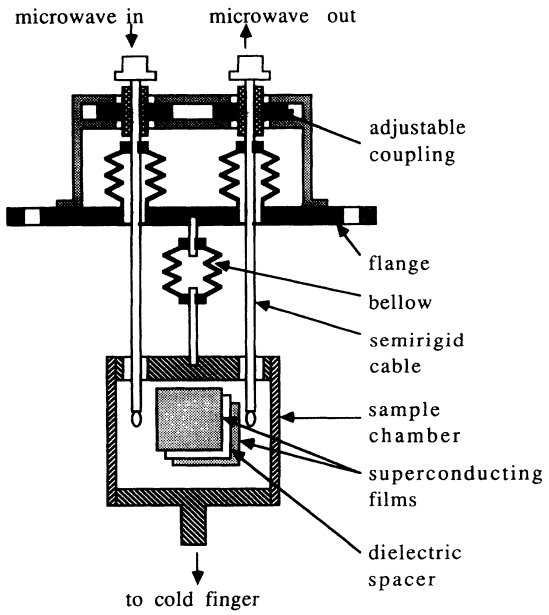


FIG. 1. Experimental setup.

The sample chamber was attached to the cold finger of a closed-cycle refrigerator. We found that the vibrations inherent to this method of cooling did not interfere with measurements. The experiments were performed under a pressure of $10^{-5}$ Torr and in a temperature range from 30 to 84 K (at higher temperatures the signal disappears due to an increase of the surface resistance near $T_c$). The temperature was measured by a platinum resistor which was attached to the copper sample chamber. The temperature difference between the sample and sample chamber did not exceed 2 K. The temperature was stabilized by the Lakeshore-330 Autotuning Temperature Controller. The magnetic field of up to 0.8 T was produced by an electromagnet which was mounted outside the sample chamber. The microwave measurements were done using an HP-83623A synthesized sweeper and an HP-8473C crystal detector. The coupling could be varied by moving the semirigid probes soldered to the bellows. All the measurements were done under computer monitoring. At each value of temperature and magnetic field the resonance curve of the PPR was measured. Using on-line fitting procedure the $Q$ factor and the resonant frequency of the PPR were determined and the surface resistance and reactance were calculated using Eq. (7). The incident power was chosen as low as possible ($-15$ dBm) in order to be in the linear regime. Upon increasing the temperature or applying a magnetic field the incident power was automatically adjusted in order to maintain a constant output signal. The resonator was always undercoupled, therefore, such a procedure maintains a constant amplitude of the microwave current in the resonator. The magnetic field was changed by steps of 0.05 T and the sample was kept at each field level for one minute, so that the whole field sweep at fixed orientation took about 20 min. Then the electromagnet was rotated (it was the only manual operation in the whole measurement) and the field sweep was repeated for the next orientation of the field. The rotation of the electromagnet was done in such a way that the dc magnetic field was always perpendicular to the microwave current. There was no appreciable difference in results for the zero-field cooled sample and for the field-cooled sample except at low fields (less than 0.1 T).

The measurements were performed on three pairs of laser-ablated $10\times10$ mm$^2$ $YBa_2Cu_3O_{7-x}$ films on sapphire or MgO substrates received from Synergy Superconductive Technologies, Ltd., Israel, and on one pair of $3\times10$ mm$^2$ $YBa_2Cu_3O_{7-x}$ films on $LaAlO_3$ prepared by the "on-axis" rf sputtering in the Royal Institute of Technology, Stockholm. The thickness of the films is 300 nm. The results obtained with these four film pairs were consistent and reproducible.

## III. EXPERIMENTAL RESULTS

### A. Field dependence

Figure 2 demonstrates the temperature dependence of the surface resistance $R_s$ and penetration depth $\lambda$ of a

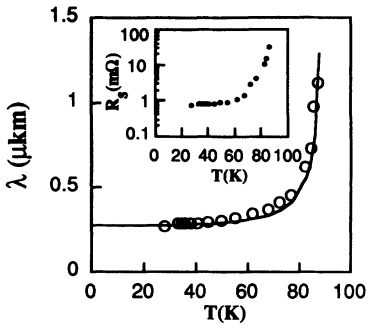


FIG. 2. Temperature dependence of the penetration depth λ of a pair of laser-ablated $YBa_2Cu_3O_{7-x}$ films at $f=5.4$ GHz calculated from Eq. (6). The solid line is the two-fluid dependence $\lambda=\lambda_0[1-(T/T_c)^4]^{-1/2}$ with $T_c=89$ K and $\lambda_0=0.27$ μkm. Inset shows temperature dependence of the surface resistance $R_s$.

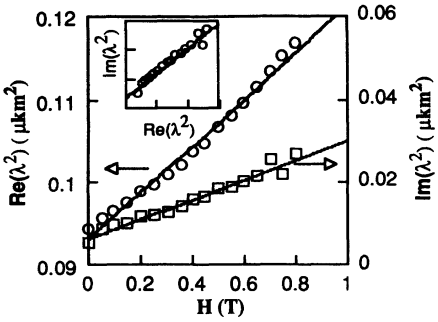


FIG. 4. Magnetic-field dependence of the real and imaginary parts of the complex penetration depth λ. Continuous lines show linear approximation. Inset shows $\mathrm{Im}(\lambda^2)$ vs $\mathrm{Re}(\lambda^2)$. The slope of this dependence yields $\omega/\omega_0$. $T=55$ K, $H\|c$.

pair of $YBa_2Cu_3O_{7-x}$ films at 5.5 GHz and in the absence of magnetic field. Here, $R_s$ is defined using Eq. (7). Figure 3 demonstrates the field dependence of the surface resistance $R_s$ and surface reactance $X_s=\mu_0\omega\,\mathrm{Re}(\lambda)$ for the same pair of $YBa_2Cu_3O_{7-x}$ films and for different orientations of magnetic field relative to the $c$ axis. Both $R_s$ and $X_s$ increase with field. The effect of magnetic field is strongest when $H\|c$ and weakest when $H\perp c$.

The pinning constant $\alpha$, viscosity $\eta$, and depinning frequency $\omega_0$ were determined as follows. First, we measured the temperature dependence of the resonant frequency and $Q$ factor of PPR without magnetic field and found the penetration depth $\lambda(T)$ using Eq. (6) (Fig. 2). Since we measure only frequency shifts, we have to estimate $\lambda(T=0)$. We evaluated $\lambda(0)$ from the fit of $\lambda(T)$ to the two-fluid model. Then we measured the resonant frequency and $Q$ factor of the resonator at several temperatures in the presence of magnetic field and determined the penetration depth $\lambda(H,T)$ in magnetic field. We found that the dependence of both $\mathrm{Re}(\lambda^2)$ and $\mathrm{Im}(\lambda^2)$ on $H$ is close to linear at $H>0.1$ T (Fig. 4) in accordance with

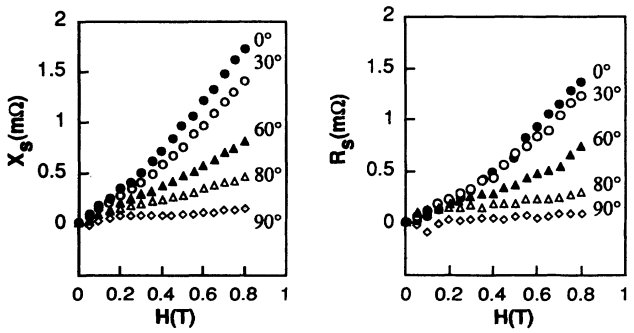


FIG. 3. Magnetic-field dependence of the surface resistance $R_s$ and surface reactance $X_s$ of the laser-ablated $YBa_2Cu_3O_{7-x}$ films at different angles between the field and $c$ axis. $T=57$ K, $f=5.4$ GHz. Only field-dependent parts of $R_s$ and $X_s$ are shown.

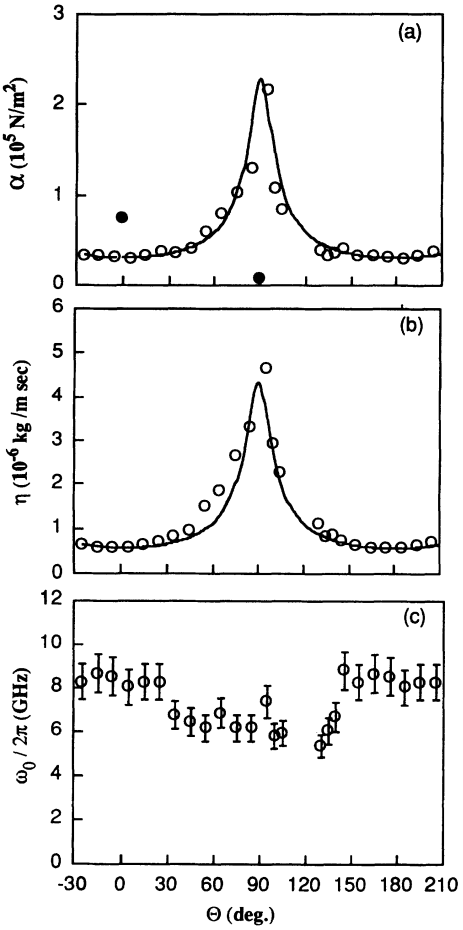


FIG. 5. Angular dependence of the pinning constant $\alpha$, viscosity $\eta$, and depinning frequency $\omega_0/2\pi$ at $T=57$ K and 0.1 T $<H<0.8$ T. Θ is the angle between the field and $c$ axis. The solid lines show approximations $\alpha(\Theta)=\alpha(0°)/\epsilon(\Theta)$, $\eta(\Theta)=\eta(0°)/\epsilon(\Theta)$, $\epsilon(\Theta)=[\cos^2(\Theta)+\gamma^{-2}\sin^2(\Theta)]^{1/2}$, and $\gamma=7.5$. Full symbols in (a) demonstrate the data of Wu and Sridhar (Ref. 14) for a $YBa_2Cu_3O_{7-x}$ single crystal at $T=57$ K and $H\le 0.1$ T.

previous observations in higher field.[12,13] This observation suggests that $\alpha$, $\eta$, and $\omega_0$ are almost field independent for $0.1\ T<H<0.8$ T [see Eq. (8)]. A small nonlinearity at low field $H<0.1$ T (Fig. 4) might be related to the vicinity of $H_{c1}$ and to the difference between $B$ and $H$. Using Eq. (8c) we find the field-independent $\omega_0$ from the slope of $\mathrm{Im}(\lambda_v^2)$ vs $\mathrm{Re}(\lambda_v^2)$ (see inset to Fig. 4). Using this value of $\omega_0$ and Eq. (8a), we find the field-independent pinning constant $\alpha$ from the slope of $\mathrm{Re}(\lambda^2)$ vs $H$ (Fig. 4). Then the viscosity $\eta$ was found from Eq. (3).

### B. Angular dependence

Figure 5 demonstrates the angular dependence of $\alpha$, $\eta$, and $\omega_0$. We note that the angular dependences of $\alpha$ and $\eta$ are very similar, while $\omega_0$ is fairly angular independent. The viscosity and pinning constant exhibit maximum values when $H\perp c$ and minimum values when $H\|c$. The same angular dependences were obtained at other temperatures and for other films. Note the different anisotropy of the pinning constant for thin films obtained in the present experiment ($\alpha_\perp/\alpha_\| \approx 7.5$) and in the experiment of Wu and Sridhar[14] for single-crystals ($\alpha_\perp/\alpha_\| \approx 0.1$).

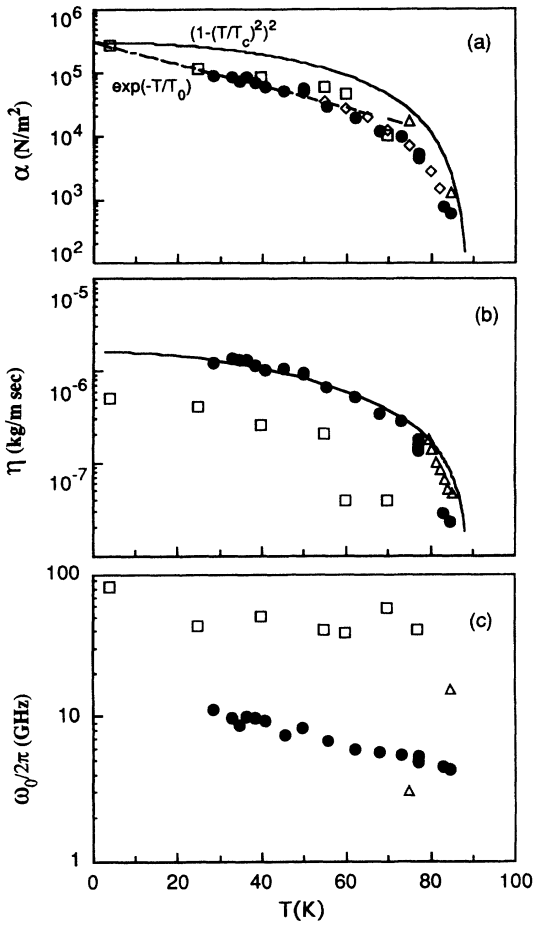


FIG. 6. Temperature dependence of the (a) pinning constant $\alpha$, (b) viscosity $\eta$, and (c) depinning frequency $\omega_0$ for $H\|c$. ●—present experiment (thin films, $f=5.5$ GHz, $0.1\ T<H<0.8$ T), □—Pambianchi *et al.* (Ref. 11) (thick films, $f=11$ GHz, $H\le 0.35$ T), ◇—Hebard *et al.* (Ref. 13) (thin films, $f=1.25$ kHz, $1\ T<H<14$ T), △—Owliaei *et al.* (Ref. 8) (thin films, $f=10$ GHz, $H<8$ T). The solid line in (a) demonstrates the approximation $\alpha(t)=3\times10^5[1-(T/T_c)^2]^2$ (N/m$^2$) with $T_c=89$ K, while the dashed straight line demonstrates the exponential dependence $\alpha(t)=3\times10^5\exp(-T/T_0)$ (N/m$^2$) with $T_0=25$ K. The solid line in (b) demonstrates the approximation $\eta(t)=1.6\times10^{-6}(1-t^2)/(1+t^2)$ (kg/m sec), where $t=T/T_c$ and $T_c=89$.

### C. Temperature dependence

Figure 6 demonstrates the temperature dependence of the pinning constant, viscosity and depinning frequency at $H\gg H_{c1}$ as found in the present work, as well as the data of other experimentalists. The pinning constant and viscosity strongly decrease with increasing temperature while the depinning frequency is only weakly temperature dependent. A remarkable observation from Fig. 6(a) is that the values of the pinning constant obtained by various methods and with different $YBa_2Cu_3O_{7-x}$ materials are very close despite the enormous differences in the measuring frequency and magnetic field (we do not plot here the pinning constant values found in the work of Wu and Sridhar[14] because their data were obtained at low fields, $H\approx H_{c1}$, and may be determined by a different pinning mechanism).

## IV. DISCUSSION

### A. Angular dependence

The angular dependences of the pinning constant and viscosity (Fig. 5) are in good agreement with the scaling model.[20] This model maps the angular-dependent properties of a uniaxial anisotropic superconductor in the mixed state ($H_{c1}\ll H\ll H_{c2}$) to the isotropic case by means of replacing the magnetic field at an arbitrary angle $\Theta$ by a reduced field $h=H\epsilon(\Theta)$. Here, $\epsilon(\Theta)=[\cos^2(\Theta)+\gamma^{-2}\sin^2(\Theta)]^{1/2}$, $\Theta$ is the angle between the field and the anisotropy axis, $\gamma$ is the anisotropy parameter. Using this scaling approach we recast Eq. (8) in terms of the reduced field and obtain

$$\lambda_v^2(H,\Theta)=\lambda_v^2(h)=\frac{h\Phi_0}{\mu_0\alpha'(h)(1+i\omega/\omega_0'(h))}\ , \tag{9}$$

where $\alpha'(h)=\alpha(H,0°)$ and $\omega_0'(h)=\omega_0(H,0°)$. We note that if $\omega_0'$ is field independent (e.g., $\omega_0'(H,0°)=\text{const}$) the scaling approach [Eq. (9)] predicts that $\omega_0$ should be angular independent (e.g., $\omega_0(H,\Theta)=\text{const}$). Indeed, we observe that $\omega_0$ is almost field independent (see linear dependence in the inset in Fig. 4) and is almost orientation independent [see Fig. 5(c)].

The experiment yields $\lambda_v^2(H,0°)\propto H$ (Fig. 4). Then Eq. (9) yields $\lambda_v^2(h)\propto h/\alpha'$ where $\alpha'$ is field independent. Therefore, $\lambda_v^2(H,\Theta)\propto H\epsilon(\Theta)/\alpha(0°)$, or, in other terms, $\alpha(\Theta)=\alpha(0°)/\epsilon(\Theta)$ in good agreement with the experiment [Fig. 5(a)]. In the same way we find $\eta(\Theta)=\eta(0°)\epsilon(\Theta)$ which agrees well with experiment [Fig. 5(b)]. The anisotropy constant $\gamma\approx 7.5$ found in our study is in good agreement with other experiments.[18,26]

The angular dependence of $\alpha$ and $\eta$ (for 30 K $< T <$ 80 K) found in the present experiment is in good agreement with the angular dependence of the microwave absorption near $T_c$ (which is determined by viscosity and pinning as well) in $YBa_2Cu_3O_{7-x}$ and $Bi_2Sr_2CaCu_2O_8$ single crystals.[18] However, the anisotropy of the pinning constant as obtained in the present experiment is in striking contradiction to the 6-MHz results of Wu and Sridhar[14] for $YBa_2Cu_3O_{7-x}$ single crystals. Specifically, they find $\alpha_\parallel/\alpha_\perp \approx \gamma$, while we find $\alpha_\parallel/\alpha_\perp \approx 1/\gamma$. The difference between these results may originate from the fact that the experiments of Ref. 14 are performed at a low field $H \leq 0.1$ T, at which $H \approx H_{c1}$, while our data are collected at a higher field $H \leq 1$ T, at which $H \gg H_{c1}$. We note that the pinning mechanism at low fields may be different from that at higher fields (for example, the low-field pinning constant may be determined by surface barriers[27]). We note also that in the limit $H \approx H_{c1}$ the scaling model[20] does not hold.

### B. Temperature dependence

#### 1. Pinning constant

An upper limit of the pinning constant $\alpha_{max}$ may be obtained by equating the energy density per unit length of the vortex core, $H_c^2\xi^2/8\mu_0$, to the elastic stored energy $\alpha_{max}\xi^2/2$.[13,14] Then

$$\alpha(t)=\frac{H_c^2(t)}{4\mu_0}=\frac{H_c^2(0)(1-t^2)^2}{4\mu_0} . \tag{10}$$

A thermodynamic estimate[28] yields $H_c(0)=1.2$ T. Then Eq. (10) yields $\alpha_{max}(t)=\alpha_0(1-t^2)^2$ with $\alpha_0=3\times10^5$ (N/m$^2$). This dependence is plotted on Fig. 6(a). At lowest temperatures the experimental data approach this upper limit while at higher temperatures the experimental data points lie lower than the model curve predicted by Eq. (10). In contrast to the previous conjectures[13,14] we conclude that the experimental data are not well fitted by the temperature dependence given by Eq. (10) even with variable $H_c$. In fact, at $T < 60$ K all the data are much better described by an exponential dependence $\alpha \propto \exp(-T/T_0)$ where $T_0 \approx 25$ K. Similar exponential dependence on temperature with the same value of $T_0$ was observed earlier for the critical current $J_c(T)$ in $YBa_2Cu_3O_{7-x}$ single crystals.[29] This exponential dependence has a nice theoretical explanation that takes into account the smearing of the pinning potential by thermal fluctuations.[2]

We note that simultaneous measurements of the pinning constant and of the critical current may reveal pinning length $r_p$ (radius of the action of the pinning potential). In fact, for the sinusoidal pinning potential $U=U_0\sin(x/r_p)$ the pinning constant $\alpha=d^2U/dx^2$, is directly related to the critical current, $J=\Phi_0^{-1}dU/dx$, as follows, $J_c=\alpha r_p/\Phi_0$. Following Ref. 30 we invert this expression and estimate $r_p$. Taking $\alpha \approx 3\times10^5\exp(-T/25)$ N/m$^2$ [the data of Fig. 6(a) at $T < 60$ K] and $J_c \approx 2.7\times10^6\exp(-T/26)$A/cm$^2$ (Ref. 29), we find $r_p \approx 2$ Å which is of the same order of magnitude as the radius of the vortex cross section (coherence length in the $a$-$b$ plane, $\xi \approx 20$ Å). This value of the pinning length is much smaller than the distance between vortices in the field of $H=1$ T, e.g., $r_p \ll (\Phi_0/H)^{1/2} \approx 45$ Å. That validates the individual vortex approximation assumed in Eqs. (1) and (8) above. The fact that the temperature dependences of the pinning constant and of the critical current at low temperatures are very similar suggests that the pinning length might be temperature independent at $T < 60$ K. The anisotropy of the pinning length may be also estimated using such analysis. For example, we compare anisotropy of the pinning constant as found in our present experiments ($\alpha_\perp/\alpha_\parallel \approx 7.5$, $T=30$–$80$ K, $H < 0.8$ T) with the anisotropy of critical current as found by Walkenhorst *et al.*[31] ($J_{c\perp}/J_{c\parallel} \approx 4$, $T=30$–$50$ K, $H=1$–$4$ T) and conclude that $r_{p\perp}/r_{p\parallel} \approx 0.5$. Of course, these estimates are very rough and to do precise ones it is necessary to measure the pinning constant and the critical current on the same sample.

#### 2. Viscosity

Our experimental data [Fig. 6(b)] are well described by the Bardeen-Stephen expression $\eta=\Phi_0H_{c2}/\rho_n$ assuming $H_{c2}(t)=100\ \mathrm{T}(1-t^2)/(1+t^2)$ and temperature-independent $\rho_n=11\ \mu\Omega$ cm. This value is smaller than the dc resistivity just above $T_c$ [$\rho_n=(50$–$100)\mu\Omega$ cm] and may indicate an increase of the quasiparticle relaxation time $\tau$ in the superconducting state.[32,33] The spread of the viscosity values as obtained in different experiments [Fig. 6(b)] may be related to the spread of $\tau$ values in different materials or to the vortex Hall effect.[3,17]

#### 3. Depinning frequency

Using the Bardeen-Stephen approximation for the viscosity, Eq. (10) for the pinning constant, and the relation $H_{c2}=4\pi\lambda^2H_c^2/\Phi_0$, we estimate the depinning frequency as follows:

$$\omega_0=\frac{\beta(t)\rho_n}{16\pi^2\lambda^2}\approx\frac{\beta(t)n_s(t)}{4\tau(t)n_0} , \tag{11}$$

where $\beta(t)=\alpha/\alpha_{max}$, $\alpha_{max}$ is the maximium pinning constant [Eq. (10)], $\tau$ is the quasiparticle relaxation time, $n_s(t)$ is the concentration of the Cooper pairs, and $n_0$ is the carrier concentration in the normal state. The temperature dependence of $\omega_0$ as given by Eq. (11) is governed by interplay between the temperature dependences of $\beta$, $\tau$, and $n_s$. The account for the activation processes[25,34] (flux creep) also leads to the temperature dependence of $\omega_0$. However, the activation processes in good $YBa_2Cu_3O_{7-x}$ materials in the fields of 1–10 T are dominant only at several degrees below $T_c$,[34] in the range where the individual vortex approach of Gittleman and Rosenblum [Eq. (1)] does not hold due to the vicinity of the vortex-solid–vortex-liquid transition and the importance of collective effects.[3,35,36] Therefore, we do not discuss here experimental data above 80 K. The available experimental data do not demonstrate strong temperature dependence of $\omega_0$ in $YBa_2Cu_3O_{7-x}$ films [Fig. 6(c)].

TABLE I. Vortex depinning frequency in type-II superconductors.

| Material | $T$ (K) | $\omega_0/2\pi$ (Hz) | Magnetic field | Method | Ref. |
|---|---|---|---|---|---|
| Pb-In | 1.7 | $7\times10^6$ | | Rf absorption | 1 |
| Nb-Ta | 4.2 | $2.6\times10^7$ | | Rf absorption | 1 |
| $Nb_3Sn$ | 1.7 | $>3\times10^8$ | | Rf absorption | 1 |
| Nb (annealed) | 1.96 | $<10^6$ | | Calorimetry | 4 |
| Nb (rolled) | 1.96 | $\sim10^8$ | | Calorimetry | 4 |
| $(BEDT\text{-}TTF)_2$-$Cu(NCS)_2$ single crystal | 4.2–9.9 | $6\times10^7$ [a] | | Rf-penetration length; estimate from the Coffey-Clem model | 37 |
| Nd-Ce-Cu-O thin film | 5–20 | $10^{10}$–$10^{11}$ [a] | 0.5–2.5 T | Microwave absorption; estimate from the Coffey-Clem model | 15 |
| $Tl_2Ca_2BaCu_2O_8$ single crystal | 76 | $\sim4\times10^{11}$ [a] | 0.6 T | Microwave absorption; estimate from the Coffey-Clem model | 9 |
| $Bi_2Sr_2Ca_1Cu_2O_8$ single crystal | 70–80 | $\sim4\times10^{10}$ [a] | 0.2–0.4 T | Microwave absorption; estimate from the Coffey-Clem model | 10 |
| $YBa_2Cu_3O_{7-x}$ thick film | 4.2–80 | $\sim4\times10^{10}$ | $<0.35$ T | Direct microwave measurements | 11 |
| $YBa_2Cu_3O_{7-x}$ thin-film stripline | 4.3 | $(2\text{–}4)\times10^{10}$ | $<6$ T | Direct microwave measurements | 12 |
| $YBa_2Cu_3O_{7-x}$ thin film | 30–80 | $(0.5\text{–}1)\times10^{10}$ | $<0.8$ T | Direct microwave measurements | Our study |

[a]The estimate *a priori* assumes field-independent pinning constant and viscosity coefficient and is crucially dependent on the applicability of the Coffey-Clem model (Ref. 25).

This might be evidence for the temperature-dependent quasiparticle relaxation time $\tau(t)$ which compensates for the temperature dependence of $n_s$ and $\beta$. We note that measurements on organic superconductors[37] also suggest temperature-independent $\omega_0$.

Under the assumption of zero temperature and maximum pinning strength ($\beta=1$, $n_s=n_0$) the depinning frequency is directly related to the quasiparticle scattering time, $\omega_0\approx\frac{1}{4}\tau$. In Table I we compare depinning frequencies for different superconductors. We observe that the depinning frequencies of low-$T_c$ superconductors are two orders of magnitude smaller than those of high-$T_c$ ones and that may be related to the low relaxation time of the latter. From the application viewpoint it means that the magnetic-field-induced losses in high-$T_c$ superconductors in the microwave range are substantially smaller than those for low-$T_c$ ones. Taking into account the high critical field of the high-$T_c$ superconductors it means that high-$Q$ resonators prepared from these materials may work in magnetic fields unlike their Nb counterparts.

## V. CONCLUSIONS

(1) The angular dependences of the vortex viscosity and pinning constant in $YBa_2Cu_3O_{7-x}$ thin films are the same in contrast to the experimental results in single crystals.[14] The viscosity and pinning constant are the lowest when $H\|c$ and the highest when $H\perp c$. The angular dependences obtained in the present work are well described by the scaling model.[20]

(2) The depinning frequency in $YBa_2Cu_3O_{7-x}$ thin films is angular independent and weakly depends on temperature.

(3) The values of the pinning constant as obtained in different works and for different $YBa_2Cu_3O_{7-x}$ material are very close. The pinning constant is close to its upper limit at lowest temperatures and decreases exponentially with increasing temperature. Comparison with the critical current density reveals the pinning length.

(4) The temperature dependence of viscosity is well described by the Bardeen-Stephen expression with reduced normal-state resistivity.

## ACKNOWLEDGMENTS

We greatly benefited from the discussions with M. V. Feigelman, V. Vinokur, A. I. Larkin, V. B. Geshkenbein, E. B. Sonin, and L. Burlachkov. We are grateful to A. M. Portis who inspired this research and to S. Revenaz and D. Oates for the communication of their results prior to publication. We thank R. C. Taber for helpful advice concerning construction of the parallel-plate resonator. We are grateful to S. Chocron, E. Iskevitch, and B. Brodskii from Synergy Superconductive Technologies Ltd., Jerusalem, Israel for the laser-ablated films. We are obliged to K. V. Rao and A. Grishin from the Royal Institute of Technology, Stockholm for rf-sputtered films. The work was supported by the Klatchkin foundation, the NiederSachsen-Jerusalem collaboration, the Israeli Ministry of Science and Arts, and the European Community.

[1]J. I. Gittleman and B. Rosenblum, Phys. Rev. Lett. **16**, 734 (1966).
[2]M. V. Feigelman and V. M. Vinokur, Phys. Rev. B **41**, 8986 (1990); A. E. Koshelev and V. M. Vinokur, Physica C **173**, 465 (1991).
[3]C. J. van der Beek, V. B. Geshkenbein, and V. M. Vinokur Phys. Rev. B **48**, 3393 (1993).
[4]J. le G. Gilchrist and P. Monceau, Philos. Mag. **18**, 237 (1968).
[5]R. Marcon, R. Fastampa, M. Giura, and E. Silva, Phys. Rev. B **43**, 2940 (1991).
[6]E. Silva, R. Marcon, and F. C. Matacotta, Physica C **218**, 109 (1993).
[7]M. X. Huang, S. M. Bhagat, A. T. Findikoglu, T. Venkatesan, M. A. Manheimer, and S. Tyagi, Physica C **193**, 421 (1992).
[8]J. Owliaei, S. Sridhar, and J. Talvacchio, Phys. Rev. Lett. **69**, 3366 (1992).
[9]N. H. Tea, M. B. Salamon, T. Datta, H. M. Duan, and A. M. Hermann, Phys. Rev. B **45**, 5628 (1992).
[10]F. Zuo, M. B. Salamon, E. D. Bukowski, J. P. Rice, and D. M. Ginsberg, Phys. Rev. B **41**, 6600 (1990).
[11]M. S. Pambianchi, D. H. Wu, L. Ganapathi, and S. M. Anlage, IEEE Trans. Appl. Supercond. **3**, 2774 (1993).
[12]S. Revenaz, D. E. Oates, D. Labbe-Lavigne, G. Dresselhaus, and M. Dresselhaus (unpublished).
[13]A. F. Hebard, P. L. Gammel, C. E. Rice, and A. F. J. Levi, Phys. Rev. B **40**, 5243 (1989).
[14]D. H. Wu and S. Sridhar, Phys. Rev. Lett. **65**, 2074 (1990).
[15]N. C. Yeh, U. Kriplani, W. Jiang, D. S. Reed, D. M. Strayer, J. B. Barner, B. D. Hunt, M. C. Foote, R. P. Vasquez, A. Gupta, and A. Kussmaul, Phys. Rev. B **48**, 9861 (1993).
[16]M. Golosovsky, Y. Naveh, and D. Davidov, Phys. Rev. B **45**, 7495 (1992).
[17]Y. Matsuda, N. P. Ong, Y. F. Yan, J. M. Harris, and J. B. Peterson (unpublished).
[18]M. Golosovsky, V. Ginodman, D. Shaltiel, W. Gerhouser, and P. Fischer, Phys. Rev. B **47**, 9010 (1993).
[19]R. C. Haddon, S. H. Glarum, S. V. Chichester, A. P. Ramirez, and N. M. Zimmerman, Phys. Rev. B **43**, 2642 (1991).
[20]G. Blatter, V. B. Geshkenbein, and A. I. Larkin, Phys. Rev. Lett. **68**, 875 (1992).
[21]R. A. Klemm, Phys. Rev. B **47**, 14 630 (1993).
[22]Z. Hao and J. R. Clem, Phys. Rev. B **46**, 5853 (1992); **43**, 7622 (1991).
[23]V. G. Kogan and J. R. Clem, Phys. Rev. B **24**, 2497 (1981).
[24]R. C. Taber, Rev. Sci. Instrum. **61**, 2200 (1990).
[25]M. W. Coffey and J. R. Clem, Phys. Rev. Lett. **67**, 386 (1991).
[26]D. E. Farrell, J. P. Rice, D. M. Ginsberg, and J. Z. Liu, Phys. Rev. Lett. **64**, 1573 (1990); M. Yethiraj, H. A. Mook, G. D. Wignall, R. Cubitt, E. M. Forgan, S. L. Lee, D. M. Paul, and T. Armstrong, *ibid.* **71**, 3019 (1993).
[27]L. Burlachkov, Phys. Rev. B **47**, 8056 (1993).
[28]M. B. Salamon and J. Bardeen, Phys. Rev. Lett. **59**, 2615 (1987).
[29]V. A. Larkin, Ph.D. thesis, Chernogolovka, Institute of Solid State Physics, 1992.
[30]R. A. Doyle, A. M. Campbell, and R. E. Somekh, Phys. Rev. Lett. **71**, 4241 (1993).
[31]A. Walkenhorst, C. Tome-Rosa, S. Stolzel, G. Jacob, M. Schmitt, and H. Adrian, Physica C **177**, 165 (1991).
[32]D. A. Bohn, R. Liang, T. M. Riseman, D. J. Baar, D. C. Morgan, K. Zhang, P. Dosanjh, T. L. Duty, A. MacFarlane, G. D. Morris, J. H. Brewer, W. N. Hardy, C. Kallin, and A. J. Berlinsky, Phys. Rev. B **47**, 11 314 (1993).
[33]F. Gao, J. W. Kruse, C. E. Platt, M. Feng, and M. V. Klein, Appl. Phys. Lett. **63**, 2274 (1993).
[34]H. A. Blackstead, D. B. Pulling, and C. A. Clough, Phys. Rev. B **44**, 6955 (1991).
[35]H. K. Olsson, R. H. Koch, W. Eidelloth, and R. P. Robertazzi, Phys. Rev. Lett. **66**, 2661 (1991).
[36]H. Wu, N. P. Ong, and Y. Q. Li, Phys. Rev. Lett. **71**, 2642 (1993).
[37]S. Sridhar, B. Maheswaran, B. A. Willemsen, D. H. Wu, and R. C. Haddon, Phys. Rev. Lett. **68**, 2220 (1992).

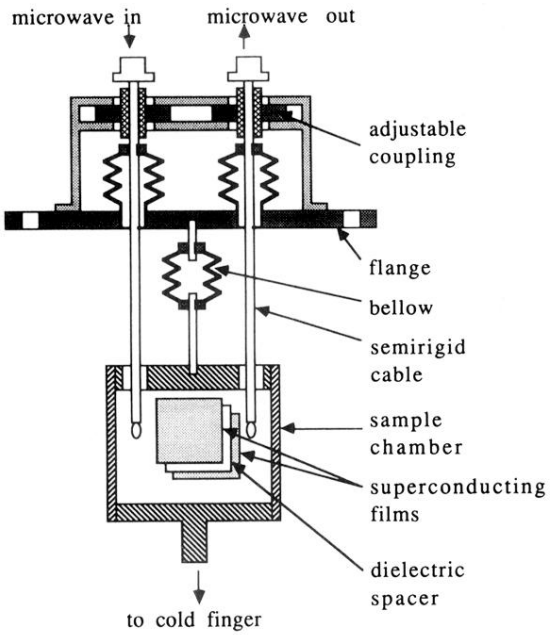


FIG. 1. Experimental setup.